ORIGINAL

Effect of daikenchuto (TU-100) on carcinogenesis in non-alcoholic steatohepatitis

Shinichiro Yamada[1], Yuji Morine[1], Satoru Imura[1], Tetsuya Ikemoto[1], Yu Saito[1], Mayuko Shimizu[2], Koichi Tsuneyama[2], Mitsue Nishiyama[3], Shiori Ishizawa[3], and Mitsuo Shimada[1]

[1]Department of Surgery, Tokushima University, Tokushima, Japan, [2]Department of Pathology and Laboratory Medicine, Tokushima University, Tokushima, Japan, [3]Tsumura Research Laboratories, Tsumura & Co., Ami, Ibaraki, Japan

Abstract : Background : Non-alcoholic steatohepatitis (NASH) is associated with a higher risk of hepatocellular carcinoma (HCC), and the importance of the gut–liver axis has been recognized in NASH-associated HCC. We investigated the effect of TU-100 on the intestinal microbiome and hepatocarcinogenesis in a NASH model. Methods : Seven-week-old Tsumura Suzuki obese diabetes mice, a model that shows the spontaneous onset of NASH and HCC, were used. They were divided into a TU-100 treated group and a control group. Mice were sacrificed at 24 and 48 weeks to evaluate hepatic steatosis, fibrosis, carcinogenesis, cytokine expression, and microbiome abundance. Results : At 24 weeks, the TU-100 group showed significantly lower expression of *IL6*, *IL1B*, and *ACTA2* mRNA in the liver ($P<0.05$). At 48 weeks, the TU-100 group showed significantly lower levels of serum alanine aminotransferase. The TU-100 group also showed a lower rate of NASH than the control group (28% vs 72% ; $P=0.1$). Tumor diameter was significantly smaller in the TU-100 group compared with that in the control group ($P<0.05$). Regarding the intestinal microbiome, the genera *Blautia* and *Ruminococcus* were increased in the TU-100 group ($P<0.05$), whereas *Dorea* and *Erysipelotrichaceae* were decreased in the TU-100 group ($P<0.05$). Conclusions : TU-100 regulates the intestinal microbiome and may suppress subsequent hepatocarcinogenesis in the NASH model. J. Med. Invest. 70 : 66-73, February, 2023

Keywords **:** *NASH, HCC, hepatocarcinogenesis, TU-100, microbiome*

INTRODUCTION

Nonalcoholic fatty liver disease (NAFLD) is known as one of the most common chronic liver disorders worldwide (1, 2). NAFLD is widely classified as nonalcoholic fatty liver (NAFL, the non-progressive subtype) and nonalcoholic steatohepatitis (NASH, the progressive subtype) (2). NASH is associated with an increased risk of progression to cirrhosis and hepatocellular carcinoma (HCC) and a high risk of liver-related morbidity and mortality (3). Therefore, clarification of the mechanisms mediating the progression of obesity-induced NASH-related HCC is an urgent issue.

Recently, the importance of the gut–liver axis was reported in NASH-related HCC. Specifically, alterations in gut microbiota influence bacterial translocation (BT), NASH progression, and HCC development by inducing cellular senescence and inflammatory cytokine secretion, such as interleukin-6 (IL-6) and interleukin-1β (IL-1β) (4), from hepatic stellate cells (HSCs) in the tumor microenvironment. Furthermore, via growth factors, matrix-remodeling factors, and chemokines (5), it was suggested that the gut–liver axis has an important role in inducing the cellular senescence of HSCs and liver carcinogenesis (6).

To elucidate the pathogenesis of NASH and develop an effective treatment, appropriate animal models are needed. Although some animal models have been reported, most are based on special diet-induced factors or genetic defects ; thus, it is difficult to determine the precise molecular mechanism of NASH on the basis of metabolic syndromes alone (7-9). Tsumura Suzuki obese diabetes (TSOD) mice represent a new polygenic model of spontaneous type 2 diabetes mellitus and moderate obesity that are particularly obvious at more than 11 weeks of age. In addition, male TSOD mice spontaneously develop NASH at 6 months and HCC at 12 months without any treatment because of obesity and type 2 diabetes (10).

Daikenchuto (TU-100), a traditional herbal medicine, is the most widely used Kampo medicine in Japan, with significant effects on ameliorating digestive motility and preventing postoperative ileus after gastrointestinal surgery (11-18). We previously reported that TU-100 prevented BT in the fasting rat (19) and a CPT-11 induced intestinal injury model (20) and reduced the upregulated expression of intestinal cytokines, including IL-1β, TNF-α, and IL-6. TU-100 maintained the diversity of the intestinal microbiome and decreased *Erysipelotrichaceae*, which was related to inflammatory conditions, such as colitis (21).

Abbreviations :
NAFLD : nonalcoholic fatty liver disease, NAFL : nonalcoholic fatty liver, NASH : non-alcoholic steatohepatitis, HCC : hepatocellular carcinoma, BT : bacterial translocation, IL-6 : interleukin-6, IL-1β : interleukin-1β, HSCs : hepatic stellate cells, TSOD : Tsumura Suzuki obese diabetes, AST : aspartate aminotransferase, ALT : alanine aminotransferase, qRT-PCR : reverse-transcriptase PCR, GAPDH : Glyceraldehyde 3-phosphate dehydrogenase, TNF-α : tumor necrosis factor-alpha, ACTA2 : alpha actin 2, CLDN1 : claudin 1, H&E : Hematoxylin and eosin, TE : Tris-EDTA, GS : glutamine synthetase, HCA : hepatocellular adenoma, α-SMA: alpha-smooth muscle actin, STAT3 : signal transducer and activator of transcription 3

Received for publication July 27, 2022 ; accepted October 12, 2022.

Address correspondence and reprint requests to Shinichiro Yamada, M.D., PhD., FACS, Department of Surgery, Tokushima University, 3-18-15 Kuramoto-cho, Tokushima 770-8503, Japan.
E-mail : yamada.shinichirou@tokushima-u.ac.jp

Furthermore, we reported that TU-100 prevented BT and directly regulated the activation of HSCs and subsequent hepatic fibrosis in a biliary atresia rat model (22). However, no report has investigated the impact of TU-100 on NASH and hepatocarcinogenesis. We hypothesize that TU-100 may prevent intestinal microbiome dysbiosis, cytokine storm in the liver, and subsequent progression of NASH and hepatocarcinogenesis. The aim of this study was to investigate the effect of TU-100 on the intestinal microbiome and hepatocarcinogenesis in a NASH model using TSOD mice.

METHODS

Experimental NASH model and TU-100 administration

Seven-week-old male TSOD mice (Institute for Animal Reproduction, Ibaraki, Japan) were used for all experiments. Mice were allowed free access to water and a basal MF diet (Oriental Yeast, Tokyo, Japan). They were housed at a temperature of 23 ± 2°C, relative humidity of 55 ± 5%, and 12-hour light/12-hour dark cycle with lights on from 0800 to 2000 hours (8 am to 8 pm) daily. They were divided into two groups : a TU-100 group (basal MF diet+TU-100) and a control group (basal MF diet only). In the TU-100 group, TU-100 (300 mg/kg/d) was administered orally every day to the end of the experiment, as reported previously (20). Body weight and blood sugar were measured at 8, 16, 24, and 48 weeks. Fecal pellets were harvested from mice at 0, 1, 4, 12, and 24 weeks. Each group had 15 mice, and at 24 (n = 8) and 48 weeks (n = 7) after TU-100 administration, the liver, the colon and blood were collected for analysis. TSOD mouse was spontaneous NASH model, and predetermined physiological or behavioral signs that define the point at which an experimental animal's pain and/or distress were not confirmed. This study was conducted in compliance with the Division for Animal Research Resources, Tokushima University. The experiments and procedures were approved by the Animal Care and Use Committee of Tokushima University (T2020-111) and performed in accordance with the NIH Guide for the Care and Use of Laboratory Animals.

Reagents

TU-100 granules were made by Tsumura & Co. (Tsumura Daikenchuto Extract Granules ; Tsumura & Co., Tokyo, Japan) under strictly controlled conditions. TU-100 contains three common medical herbs : ginseng (*Ginseng radix*, 30%), processed ginger (*Zingiberis Siccatum Rhizoma*, 50%), and Japanese pepper (*Zanthoxylum* fruit, 20%) (21).

Serum liver function test

To evaluate liver injury, the levels of serum aspartate aminotransferase (AST) and alanine aminotransferase (ALT) were measured when mice were sacrificed using the Japan Society of Clinical Chemistry standardization matching method. All measurements were performed by Shikoku Chuken, Inc., Kagawa, Japan.

Real-time PCR

Pieces of the colonic wall and non-cancerous liver specimen were homogenized, and total RNA was isolated using an RNeasy Mini Kit (Qiagen, Hilden, Germany) in accordance with the manufacturer's statement. Then, the specimens were used for quantitative analysis of gene expression using reverse-transcriptase PCR (qRT-PCR). cDNA was prepared using a reverse transcription kit (High Capacity cDNA Reverse Transcription Kits ; Applied Biosystems, Foster City, CA, USA). *GAPDH* (Applied Biosystems) was used as an endogenous control. Interleukin-1β (*IL1B*), interleukin-6 (*IL6*), and alpha actin 2 (*ACTA2*) in the liver, and claudin 1 (*CLDN1*) in the colon were assessed using TaqMan gene expression assays (*IL6*, Mm00446190_m1 ; *IL1B*, Mm00434228_m1 ; *ACTA2*, Mm00725412_s1 ; *CLDN1* ; Mm00516701_m1 : Applied Biosystems). TaqMan gene expression assays were conducted in duplicate in 20 mL reactions using TaqMan Array 96-well plates and a real-time PCR System (StepOnePlus ; Applied Biosystems) following the manufacturer's statement. Standard curves were made from three-fold serial dilutions of cDNA, and the copy numbers of target genes were calculated in accordance with the standard curves (21).

Evaluation of steatosis, fibrosis, and hepatic tumors

Formalin-fixed, paraffin-embedded liver tissues were prepared for Hematoxylin and eosin (H&E) staining and evaluated by an experienced pathologist. The degree of NASH was evaluated with the FLIP algorithm (23). The number and maximum diameter of hepatic tumors were measured from the liver surface macroscopically. The characteristics of tumors were confirmed by immunohistochemistry. All the formalin-fixed, paraffin-embedded tissues were processed, and 4-μm serial sections were cut. Immunohistochemical staining for glutamine synthetase (GS) was performed. Rabbit polyclonal anti-GS (clone GS-6 ; dilution 1 : 500 ; cat. no. MAB302 ; Millipore, CA, USA) was employed as the primary antibodies. The sections were incubated with the primary antibodies in a wet chamber for 60 min at room temperature. After rinsing with Tris-buffered saline (TBS) containing 0.1% Tween (TBS-T), the sections were incubated with EnVision Peroxidase (PO) (Dako, Tokyo, Japan) for 60 min at room temperature. After rinsing in TBS-T, 3,3'-diaminobenzidine (Sigma, Steinheim, Germany) was applied as a substrate for the PO. GS-positive tumors were defined as GS (+) HCC-like tumors, and negative tumors were classified as GS (-) hepatocellular adenoma (HCA)-like tumors (24). Microscopic observation was performed using an Olympus BX51N (Tokyo, Japan) with UPlanFL N objective lenses (10×/0.30, 20×/0.5 and 40×/0.75 ; Olympus) at room temperature, and then images were acquired using camera (DP27, Olympus) and cellSens Standard software (version 1.17.16030.0, Olympus).

16S rRNA gene metagenome sequencing of stool samples

Approximately 30 mg of stool samples were homogenized in 1 mL extraction buffer (10% 400 μL sodium dodecyl sulfate (Sigma-Aldrich Japan Inc., Tokyo, Japan) in Tris-EDTA (TE) buffer (pH 7.4 10 mmol/L Tris ; Fujifilm Waco Pure Chemical Corporation, Osaka, Japan and pH 8.0 1 mmol/L EDTA ; Fujifilm Waco Pure Chemical Corporation), 200 μL 3 M sodium acetate (Fujifilm Waco Pure Chemical Corporation), and 400 μL phenol : chloroform : isoamyl alcohol (25 : 24 : 1 v/v) (Nippon Gene, Tokyo, Japan)), added to a Lysing Matrix E Tube (MP Biomedicals, Solon, OH, USA), and homogenized using a FastPrep-24 automated cell disruptor (MP Biomedicals) for 40 sec at 6 m/sec. This procedure was performed twice. The homogenate was centrifuged for 30 min at 10,000 × g, and an extract of DNA was collected as the aqueous phase and purified by adding a matched volume of phenol : chloroform : isoamyl alcohol (25 : 24 : 1, v/v) twice. Next, an equal volume of isopropyl alcohol (Fujifilm Waco Pure Chemical Corporation) was added, and DNA was obtained as a pellet by centrifugation (5 min, 10,000 × g). After drying, the DNA was dissolved in TE. The preparation of the 16S rRNA gene metagenome library for MiSeq (Illumina, Inc., San Diego, CA, USA) was conducted in accordance with the manufacturer's instructions. Sequence data were processed using the 16S rRNA sequence analysis pipeline QIIME 1.8.0.

Statistical analysis

The Student's t test (body weight, blood sugar, and serum liver function test), unpaired Mann–Whitney U test (mRNA expression and tumor status), or chi-squared test was used to compare variables between the two groups. For all statistical analyses, $P<0.05$ was considered significant. All statistical analyses were performed using statistical software (JMP 8.0.1., SAS Campus Drive, Cary, NC, USA).

RESULTS

Evaluation of diabetes mellitus and liver function

Body weight and blood sugar showed no significant difference between the two groups at 8, 16, 24, and 48 weeks (Table 1). Furthermore, the serum levels of AST and ALT showed no significant difference between the two groups at 24 weeks (Table 2). However, at 48 weeks, ALT levels were significantly lower in the TU-100 group than in the control group ($P<0.05$) (Table 2).

Table 1. Body weight and blood sugar in the control group and TU-100 group

	Control (n=8)	TU-100 (n=8)	*P* value
Body weight (g)			
8 weeks	58.8 ± 4.5	58.1 ± 3.6	0.52
16 weeks	61.2 ± 4.7	61.4 ± 3.7	0.54
24 weeks	65.7 ± 5.5	66.5 ± 3.9	0.32
48 weeks	66.5 ± 5.9	65.2 ± 7.8	0.59
Blood sugar (mg/dl)			
8 weeks	207 ± 43	198 ± 39	0.43
16 weeks	269 ± 45	290 ± 51	0.56
24 weeks	345 ± 129	399 ± 159	0.20
48 weeks	239 ± 115	256 ± 136	0.71

All data are shown as the mean ± standard deviation and compared with Student's t test.

Table 2. Serum AST and ALT levels in the control group and TU-100 group

	Control (n=7)	TU-100 (n=7)	*P* value
AST (U/L)			
24 weeks	196 ± 120	163 ± 72	0.52
48 weeks	671 ± 478	390 ± 188	0.17
ALT (U/L)			
24 weeks	104 ± 51	100 ± 33	0.86
48 weeks	162 ± 31	111 ± 44	0.03

All data are shown as the mean ± standard deviation and compared with Student's t test. AST : aspartate aminotransferase, ALT : alanine aminotransferase

Cytokine expression in the liver (RT-PCR)

Figure 1A shows the mRNA expression levels of cytokines at 24 weeks after the administration of the basal MF diet with or without TU-100. The mRNA expression of *ACTA2* (α-SMA) in the liver was significantly suppressed in the TU-100 group compared with that in the control group ($P<0.05$). The mRNA expression of the inflammatory cytokines *IL6* and *IL1B* in the liver was also suppressed in the TU-100 group compared with that in the control group ($P<0.05$). Furthermore, the mRNA expression of *CLDN1* in the colon, which is a component of intestinal tight junctions, was maintained in the TU-100 group compared with that in the control group ($P<0.05$). In contrast, *ACTA2*, *IL6*, and *IL1B* mRNA expression in the liver showed no significant difference between the two groups at 48 weeks (Figure 1B).

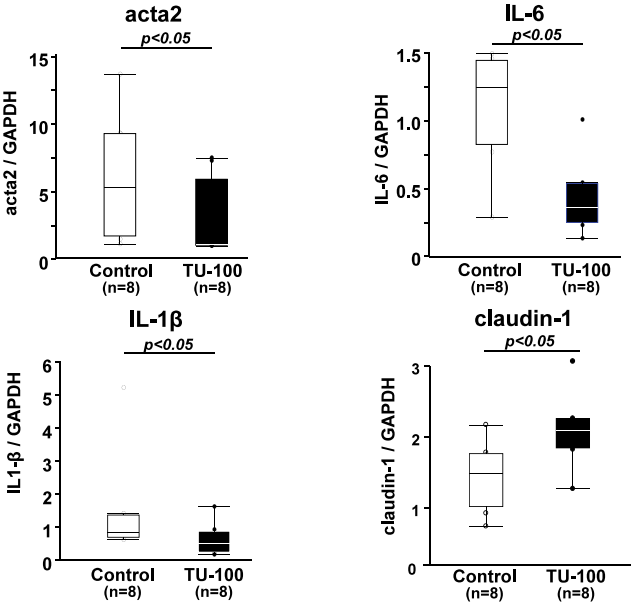

Fig 1A

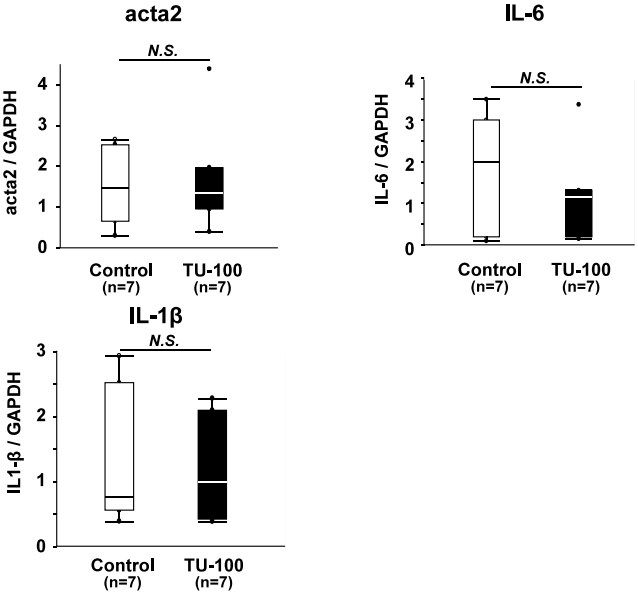

Fig 1B

Fig 1. Cytokine expression (IL-6, IL-1β, α-SMA : non-cancerous liver tissue ; claudin-1 : colonic wall) in control and TU-100 groups at 24 (A) and 48 weeks (B). Expression of the cytokines IL-6, IL-1β, and α-SMA was significantly lower in the TU-100 group compared with that in the control group. Claudin-1 expression was maintained in the TU-100 group. In contrast, IL-6, IL-1β, and α-SMA expressions in the liver showed no significant difference between the two groups. Unpaired Mann–Whitney U test was used.

Evaluation of steatosis, fibrosis, and hepatic tumors

Figure 2A shows the representative cases of H&E staining at 24 and 48 weeks. At 24 weeks, the rate of lobular inflammation (main finding of NASH) was significantly higher in the control group than in the TU-100 group (75% vs 13%, $P<0.01$) (Fig. 2B). At 48 weeks, control cases showed the typical findings of NASH, including steatosis, lobular inflammation, and ballooning. These features of NASH were suppressed by TU-100 administration. At 48 weeks, although there was no significant difference, TU-100 tended to prevent the progression of NASH, with a lower rate of NASH in the TU-100 group than in the control group (71% vs 28%, $P=0.1$) (Fig. 2C). Regarding hepatocarcinogenesis in NASH livers, there were no hepatic tumors at 24 weeks (n=8 for each group), and all mice showed tumors in the liver at 48 weeks (n=7 for each group). There was no significant difference in tumor number between the two groups. However, the maximum diameter of tumors was significantly smaller in the TU-100 group compared with that in the control group ($P<0.05$) (Fig. 2D). In the TU-100 group, GS (-) HCA-like tumors were mainly observed in one case (Fig. 2D).

Microbiome analysis

Meta 16S rRNA gene sequencing analysis of the fecal microbiota revealed no dramatic changes in phyla and genera following TU-100 administration at any time point (Fig 3). However, there were several gut microbiome species that showed a significant difference between the two groups. *Blautia* and *Ruminococcus* were increased in the TU-100 group ($P<0.05$) (Fig 4A), and the genus *Dorea* and an unknown genus of the family *Erysipelotrichaceae* were decreased in the TU-100 group ($P<0.05$) (Fig. 4B).

DISCUSSION

In our study, we identified that TU-100 regulated the intestinal microbiome and suppressed subsequent HSC activation, NASH progression, and tumor development in a NASH model. The mRNA expression of *ACTA2*, *IL6*, and *IL1B* in the liver was suppressed, whereas *CLDN1* mRNA in the colon was maintained in the TU-100 group. TU-100 tended to suppress the formation of NASH, and tumor diameters in the liver in the TU-100 group

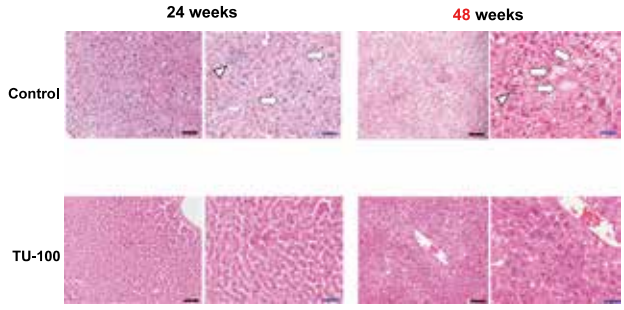

Fig 2A. Representative images of the liver at 24 and 48 weeks. The liver in the control group showed typical NASH findings, such as steatosis, lobular inflammation, and ballooning. These findings were suppressed in the liver from the TU-100 group. Arrowhead : lobular inflammation, arrow: ballooning Black scale bar : 100μm Blue : 50μm

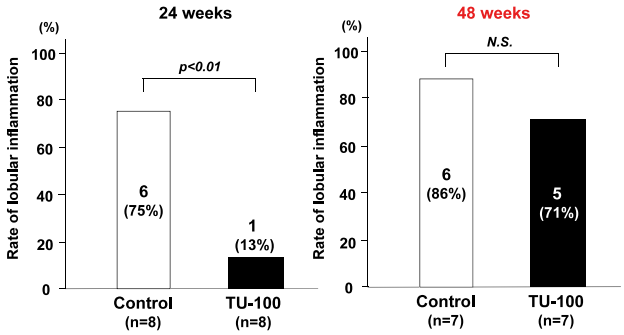

Fig 2B. The rate of lobular inflammation at 24 weeks, the main finding of NASH, was significantly higher in the control group than in the TU-100 group ($P<0.01$). There was no significant difference at 48 weeks. Chi-squared test was used.

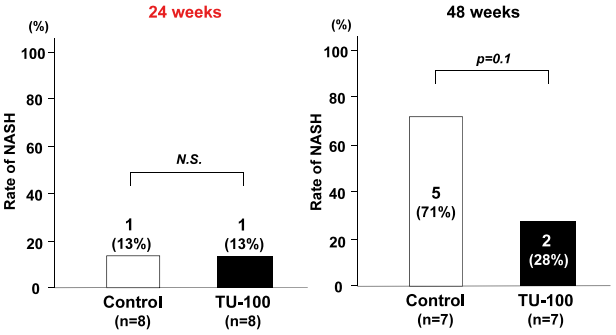

Fig 2C. The rate of NASH by the FLIP algorithm showed no significant difference at 24 weeks. It tended to be lower in the TU-100 group compared with that in the control group ($P=0.1$) at 48 weeks. Chi-squared test was used.

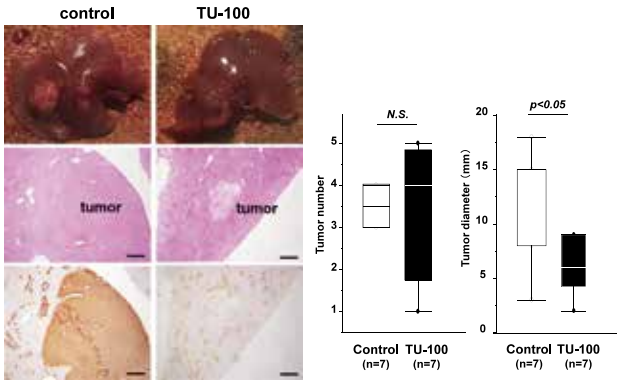

Fig 2D. Pictures of the liver at 48 weeks, tumor number, and maximum tumor diameter in control and TU-100 groups. Although tumor number showed no significant difference between the two groups, the maximum tumor diameter in the TU-100 group was significantly smaller than that in the control group ($P<0.05$).
Unpaired Mann–Whitney U test was used. GS-positive tumors were defined as HCC-like tumors, and GS-negative tumors were classified as HCA-like tumors. Scale bar: 100 μm

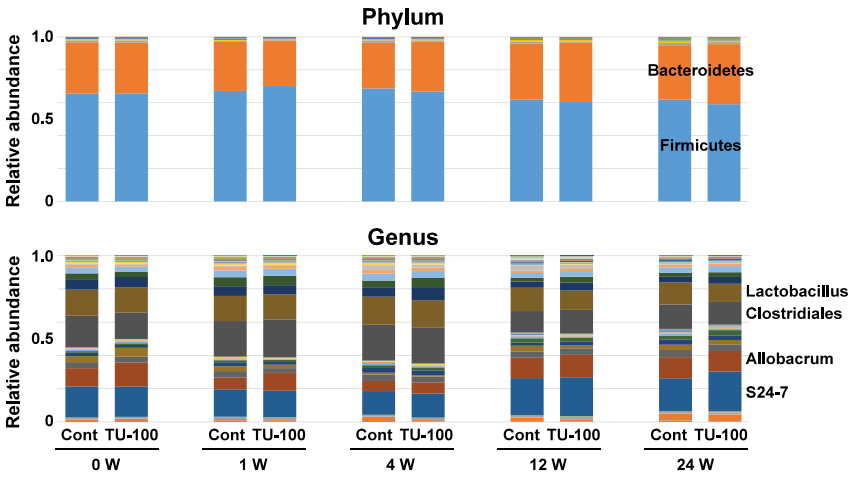

Fig 3. Meta 16S rRNA gene sequencing analysis of the fecal microbiota at 0, 1, 4, 12, and 24 weeks. Color bands in graphs indicate types of phyla and genera. Phyla and genera did not show dramatic changes after TU-100 administration at any time point.

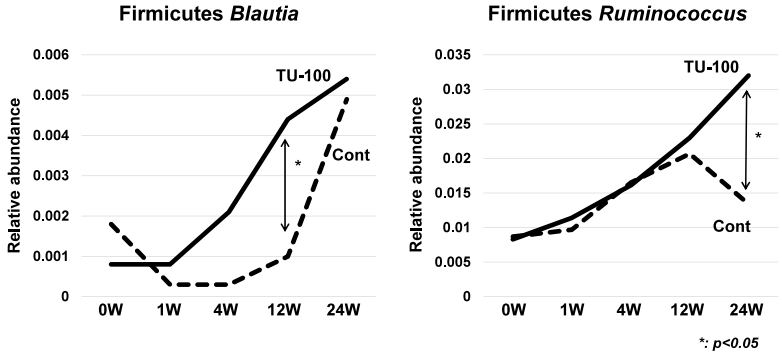

Fig 4A

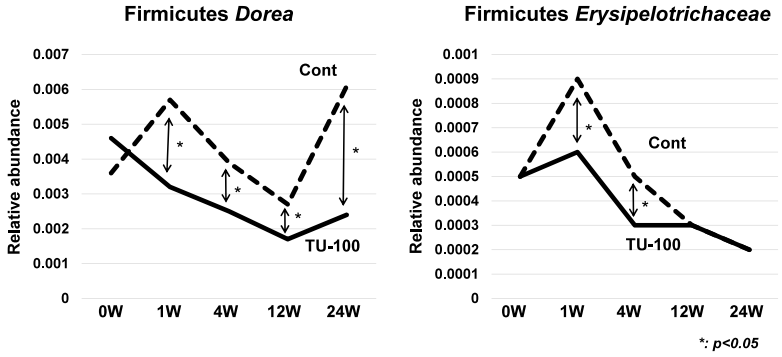

Fig 4B

Fig 4. Relative abundance of the microbiome at 0, 1, 4, 12, and 24 weeks. (A) *Firmicutes, Blautia,* and *Ruminococcus* were significantly increased in the TU-100 group compared with those in the control group ($P<0.05$). (B) *Firmicutes, Drea,* and *Erysipelotrichaceae* were significantly decreased in the TU-100 group compared with those in the control group ($P<0.05$).

were significantly smaller compared with those in the control group. Regarding the microbiome analysis, the genera *Blautia* and *Ruminococcus* were increased, and the genus *Dorea* and an unknown genus of the family *Erysipelotrichaceae* were decreased in the TU-100 group.

Although long-term infection with hepatitis B or C virus is a common risk factor for HCC, obesity-related NAFL and NASH have recently been reported as important causes of HCC (25). Because of the increased incidence of obesity-related HCC, the mechanisms involved in this disease and its prevention should be investigated. HSCs have been reported to play pivotal roles in HCC development via the secretion of inflammatory cytokines

(26), and these cytokines are influenced by gut microbial metabolites through portal flow (6). In physiologically normal conditions, HSCs exist in the space of Disse in a quiescent state and display a myofibroblast phenotype once activated (27). Activated HSCs secrete α-SMA and are the primary contributors to pathogenic extracellular matrix production in hepatic fibrosis (28).

Regarding the mouse model of NASH and hepatocarcinogenesis, we used TSOD mice in this study. This model spontaneously develops lobular inflammation and hepatocellular ballooning at 6 months and HCC at 12 months without any treatment because of obesity and type 2 diabetes (10). Takahashi *et al*. revealed that tumors in TSOD mice histologically reflect well-differentiated HCC in humans by the immunohistochemical staining of GS and β-catenin (24).

Inflammatory cytokines, including IL-6 and IL-1β, have cell-nonautonomous functions associated with inflammation and tumorigenesis promotion. IL-6 has been reported to increase NASH and cancer risk in obese individuals (29). IL-6 is a multifunctional cytokine with important functions in proliferation, apoptosis, cell survival, and immune responses (30). IL-6 produced in the liver microenvironment activates STAT-3 signaling in hepatocytes and is related to hepatocarcinogenesis (31), whereas elevated IL-6 levels have been shown to be related to HCC in human samples (32). More recently, IL-6 signaling has been identified as a pivotal pathway accelerating the expansion of liver cancer progenitors and/or cancer stem cells (33, 34). IL-1β is a pro-inflammatory cytokine and has been reported to influence the progression of NASH, similar to IL-6 (35). IL-1β was shown to be related to elevated β-catenin and its target gene *MYC* and to play a potential role in hepatocarcinogenesis. It has been also reported that inflammasome activation and subsequent IL-1β maturation acted as an upstream regulator of the induction of other inflammatory cytokines in HSCs (6). In our study, α-SMA and these inflammatory cytokines showed no significant differences between TU-100 and control groups at 48 weeks. Generally, traditional herbal medicine shows mild effects, and TU-100 appeared to have an effect at the beginning of NASH development.

The gut microbiota affects the balance between pro- and anti-inflammatory effectors in the liver and impacts NAFLD and its progression to NASH (36). Furthermore, intestinal dysbiosis promotes hepatocarcinogenesis by driving cancer-promoting liver inflammation, fibrosis, and genotoxicity (37). Intestinal dysbiosis is induced by chronic inflammation, and the bacterial diversity in non-inflammatory controls is significantly higher than that in Crohn's disease (21). We previously reported that TU-100 decreased inflammatory cytokines in the large intestine in a CPT-11 induced colitis model (38). *Blautia* and *Ruminococcus*, which were increased in the TU-100 group, are known to produce the short-chain fatty acid (SCFA) butyrate. SCFAs suppress inflammation through the regulation of immune and inflammatory cytokines (39). TU-100 was also reported to increase *Bifidobacterium*, which produces butyrate and contributes to beneficial effects on the human colon (40). Furthermore, Hasebe *et al*. showed that long-term administration of TU-100 increases the abundance of bacteria that produce SCFAs (41). In the current study, TU-100 also showed a long-term effect on *Dorea* and *Ruminococcus*. *Blautia* was associated with reduced inflammatory complications after ileal pouch-anal anastomosis (42), and butyrate ameliorated colitis development through the induction of regulatory T cell differentiation (43). Furthermore, butyrate is known as a histone deacetylase inhibitor and has been investigated as a new anticancer agent. Epigenetics, including histone deacetylation and DNA demethylation, is associated with carcinogenesis and enhanced malignant behavior (44). It was reported that the abundance of *Brautia* decreased with aging and was correlated with DNA methylation status (45). *Dorea*, which was decreased in the TU-100 group, has been reported to be elevated in NAFLD/NASH children, adolescents, and adult subjects (46). In post-menopausal obese women, *Dorea* has been shown to be related to inflammation and insulin resistance (47). These studies suggest a relationship between inflammation, obesity, and elevated *Dorea*. *Erysipelotrichaceae*, which was also decreased in the TU-100 group, has been demonstrated to be increased in high caloric diet-fed mice (48) and identified as a risk indicator of HCC in a mouse model (49). From these reports, the regulation of the microbiome by TU-100 administration may be related to the inhibition of inflammation, progression of NASH, and hepatocarcinogenesis.

We focused on the effect of TU-100 in clinical and experimental settings. We previously reported that TU-100 prevents BT in the fasting rat (19) and maintains the diversity of the gut microbiome (21). *Erysipelotrichaceae* was increased in this fasting model and the current study but decreased after TU-100 administration. Chikakiyo *et al*. (20) and Takasu *et al*. (38) reported that TU-100 suppressed the adverse effects associated with CPT-11, decreased inflammatory cytokines, improved the function of tight junctions, promoted the expression of claudin-1, and prevented BT. Furthermore, Yada *et al*. (22) reported that TU-100 decreased intestinal mucosa atrophy, BT, liver injury, hepatic fibrosis, and hepatic expression of α-SMA and TLR4 in a biliary atresia rat model. Furthermore, in an *in vitro* model, TU-100 inhibited the expression of α-SMA in HSCs. The inhibition of HSC activation appears to be mainly due to the reduced stimulation of TLR4 signaling through the prevention of BT. However, TU-100 also has direct suppressive effects on HSCs. These studies suggest that TU-100 influences intestinal inflammation, microbiome dysbiosis, and BT. HSC activation and subsequent hepatic fibrosis were also suppressed by TU-100. IL-6 and IL-1β were secreted from HSC (50), and these cytokines seemed to be decreased by suppression of HSC using TU-100. Furthermore, in the present study, we discovered that TU-100 might suppress NASH progression and subsequent hepatocarcinogenesis. To our knowledge, this is the first report on the relationship among TU-100, NASH, and hepatocarcinogenesis.

The present study has several limitations. First, the TSOD mouse model has individual differences in NASH formation because it is a model of spontaneous NASH, and some mice did not show apparent NASH in this study. A different mouse model, such as one representing the Western diet, should be investigated (51). Second, only the mRNA levels of inflammatory cytokines were measured, not their protein levels. Third, only the intestinal microbiome was investigated as the mechanism underlying the suppression of NASH and hepatocarcinogenesis by TU-100. Other detailed mechanisms should be elucidated in future studies.

In conclusion, TU-100 may suppress the progression of NASH and subsequent hepatocarcinogenesis by regulating the intestinal microbiome and HSC activation in a NASH model.

CONFLICT OF INTEREST

The authors have no financial support to disclose.

ACKNOWLEDGMENTS

We thank H. Nikki March, PhD, and Melissa Crawford, PhD, from Edanz (https://jp.edanz.com/ac) for editing a draft of this manuscript.

FUNDING

M.S received a research grant from Tsumura & Co.

AVAILABILITY OF DATA AND MATERIALS

Original data using metagenome/microbiome sequencing of stool samples is submitted as supplementary file.

AUTHOR'S CONTRIBUTION

S.Y, Y.M, S.I, T.I, Y.S, and M.S designed the study, contributed to data collection, and participated in writing the manuscript. M.S and K.T evaluated the pathological findings. M.N and S.I analyzed the intestinal microbiome.

ETHICS APPROVAL

The experiments and procedures were approved by the Animal Care and Use Committee of Tokushima University (T2020-111) and performed in accordance with the NIH Guide for the Care and Use of Laboratory Animals. The present study was conducted in compliance with the Division for Animal Research Resources, Tokushima University and performed in accordance with the NIH Guide for the Care and Use of Laboratory Animals.

COMPETING INTERESTS

M.S received a research grant from Tsumura & Co. S.Y received a reagent (TU-100) from Tsumura & Co. M.N and S.I are employed by Tsumura & Co.

Other authors declare no conflict of interests for this article.

REFERENCES

1. Younossi ZM, Koenig AB, Abdelatif D, Fazel Y, Henry L, Wymer M : Global epidemiology of nonalcoholic fatty liver disease-Meta-analytic assessment of prevalence, incidence, and outcomes. Hepatology 64 : 73-84, 2016
2. Loomba R, Sanyal AJ : The global NAFLD epidemic. Nat Rev Gastroenterol Hepatol 10 : 686-690, 2013
3. Dulai PS, Singh S, Patel J, Soni M, Prokop LJ, Younossi Z, Sebastiani S, Ekstedt M, Hagstrom H, Nasr P : Increased risk of mortality by fibrosis stage in nonalcoholic fatty liver disease : Systematic review and meta-analysis. Hepatology 65 : 1557-1565, 2017
4. Fafián-Labora J, Carpintero-Fernández P, Jordan SJD, Shikh-Bahaei T, Abdullah SM, Mahenthiran M, Rodríguez-Navarroet al J, Niklison-Chirou M, O'Loghlen A : FASN activity is important for the initial stages of the induction of senescence. Cell Death Dis 10 : 318, 2019
5. Rodier F, Campisi J : Four faces of cellular senescence. J Cell Biol 192 : 547-56, 2011
6. Yoshimoto S, Loo TM, Atarashi K, Kanda H, Sato S, Oyadomari S, Iwakura Y, Oshima K, Morita H, Hattori M : Obesity-induced gut microbial metabolite promotes liver cancer through senescence secretome. Nature 499 : 97-101, 2013
7. Anstee QM, Goldin RD : Mouse models in non-alcoholic fatty liver disease and steatohepatitis research. Int J Exp Pathol 87 : 1-16, 2006
8. Deng QG, She H, Cheng JH, French SW, Koop DR, Xiong S, Tsukamoto H : Steatohepatitis induced by intragastric overfeeding in mice. Hepatology 42 : 905-914, 2005
9. Itoh M, Suganami T, Nakagawa N, Tanaka M, Yamamoto Y, Kamei Y, Terai S, Sakaida I, Ogawa Y : Melanocortin 4 receptordeficient mice as a novel mouse model of nonalcoholic steatohepatitis. Am J Pathol 179 : 2454-2463, 2011
10. Nishida T, Tsuneyama K, Fujimoto M, Nomoto K, Hayashi S, Miwa S, Nakajima T, Nakanishi Y, Sasaki Y, Suzuki W : Spontaneous Onset of Nonalcoholic Steatohepatitis and Hepatocellular Carcinoma in a Mouse Model of Metabolic Syndrome. Lab Invest 93 : 230-41, 2013
11. Kono T, Kanematsu T, Kitajima M : Exodus of Kampo, traditional Japanese medicine, from the complementary and alternative medicines : is it time yet? Surgery 146 : 837-40, 2009
12. Manabe N, Camilleri M, Rao A, Wong BS, Burton D, Busciglio I, Zinsmeister A, Haruma K : Effect of daikenchuto (TU-100) on gastrointestinal and colonic transit in humans. Am J Physiol Gastrointest Liver Physiol 298 : G970-5, 2010
13. Iturrino J, Camilleri M, Wong BS, Linker Nord SJ, Burton D, Zinsmeister AR : Randomised clinical trial : the effects of daikenchuto, TU-100, on gastrointestinal and colonic transit, anorectal and bowel function in female patients with functional constipation. Aliment Pharmacol Ther 37 : 776-85, 2013
14. Okada K, Kawai M, Uesaka K, Kodera Y, Nagano H, Murakami Y, Morita S, Sakamoto J, Yamaue H, JAPAN-PD Investigators : Effect of Daikenchuto (TJ-100) on postoperative bowel motility and on prevention of paralytic ileus after pancreaticoduodenectomy : a multicenter, randomized, placebo-controlled phase II trial (the JAPAN-PD study). Jpn J Clin Oncol 43 : 436-8, 2013
15. Shimada M, Morine Y, Nagano H, Hatano E, Kaiho T, Miyazaki M, Kono T, Kamiyama T, Morita S, Sakamoto J : Effect of TU-100, a traditional Japanese medicine, administered after hepatic resection in patients with liver cancer : a multi-center, phase III trial (JFMC40- 1001). Int J Clin Oncol 20 : 95-104, 2015
16. Yoshikawa K, Shimada M, Wakabayashi G, Ishida K, Kaiho T, Kitagawa Y, Sakamoto J, Shiraishi N, Koeda K, Mochiki E : Effect of Daikenchuto, a traditional Japanese herbal medicine, after total gastrectomy for gastric cancer : a multicenter, randomized, double-blind, placebocontrolled, phase II trial. J Am Coll Surg 221 : 571-8, 2015
17. Kono T, Omiya Y, Hira Y, Kaneko A, Chiba S, Suzuki T, Noguchi M, Watanabe T : Daikenchuto (TU-100) ameliorates colon microvascular dysfunction via endogenous adrenomedullin in Crohn's disease rat model. J Gastroenterol 46 : 1187-96, 2011
18. Hanada K, Wada T, Kawada K, Hoshino N, Okamoto M, Hirata W, Mizuno R, Itatani Y, Inamoto S, Takahashi R : Effect of herbal medicine daikenchuto on gastrointestinal symptoms following laparoscopic colectomy in patients with colon cancer : A prospective randomized study. Biomed Pharmacother 141 : 111887, 2021
19. Yoshikawa K, Kurita N, Higashijima J, Miyatani T, Miyamoto H, Nishioka M, Shimada M : Kampo medicine "Daikenchu-to" prevents bacterial translocation in rats. Dig Dis Sci 53 : 1824-31, 2008
20. Chikakiyo M, Shimada M, Nakao T, Higashijima J, Yoshikawa K, Nishioka M, Iwata T, Kurita N : Kampo medicine "Dai-kenchu-to" prevents CPT-11-induced small-intestinal injury in rats. Surg Today 42 : 60-7, 2012
21. Yoshikawa K, Shimada M, Kuwahara T, Hirakawa H, Kurita N, Sato H, Utsunomiya T, Iwata T, Miyatani T,

Higashijima J : Effect of Kampo medicine "Dai-kenchu-to" on microbiome in the intestine of the rats with fast stress. J Med Invest 60 : 221-7, 2013
22. Yada K, Ishibashi H, Mori H, Morine Y, Zhu C, Feng R, Kono T, Shimada M : The Kampo medicine"Daikenchuto (TU-100)" prevents bacterial translocation and hepatic fibrosis in a rat model of biliary atresia. Surgery 159 : 1600-11, 2016
23. Pierre B, FLIP Pathology Consortium : Utility and Appropriateness of the Fatty Liver Inhibition of Progression (FLIP) Algorithm and Steatosis, Activity, and Fibrosis (SAF) Score in the Evaluation of Biopsies of Nonalcoholic Fatty Liver Disease. Hepatology 60 : 565-75, 2014
24. Takahashi T, Nishida T, Baba H, Hatta H, Imura J, Sutoh M, Toyohara S, Hokao R, Watanabe S, Ogawa H : Histopathological characteristics of glutamine synthetase-positive hepatic tumor lesions in a mouse model of spontaneous metabolic syndrome (TSOD mouse). Mol Clin Oncol 5 : 267-270, 2016
25. Takuma Y, Nouso K : Nonalcoholic steatohepatitis-associated hepatocellular carcinoma : our case series and literature review. World J Gastroenterol 16 : 1436-41, 2010
26. Loo TM, Kamachi H, Watanabe Y, Yoshimoto S, Kanda H, Arai Y, Nakajima-takagi Y, Iwama A, Koga T, Sugimoto Y : Gut Microbiota Promotes Obesity-Associated Liver Cancer Through PGE 2-Mediated Suppression of Antitumor Immunity. Cancer Discov 7 : 522-38, 2017
27. Farouk KE, Abeer AAS, Rehab AH : Dunaliella salina Microalgae Oppose Thioacetamide-Induced Hepatic Fibrosis in Rats. Toxicol Rep 7 : 36-45, 2019
28. Min-DeBartolo J, Schlerman F, Akare S, Wang J, McMahon J, Zhan Y, Syed J, He W, Zhang B, Martinez RV : Thrombospondin-I Is a Critical Modulator in Non-Alcoholic Steatohepatitis (NASH). PLoS One 14 : e0226854, 2019
29. Coppe´, J. P, Oatil CK, Rodier F, Sun Y, Muñoz DP, Goldstein J, Nelson PS, Desprez PY, Campisi J : Senescence-associated secretory phenotypes reveal cell-nonautonomous functions of oncogenic RAS and the p53tumor suppressor. PLoS Biol 6 : 2853-68, 2008
30. Kishimoto T : Interleukin-6 : from basic science to medicine--40 years in immunology. Annu Rev Immunol 23 : 1-21, 2005
31. Zhou M, Yang H, Marc LR, Tian H, Ling L : Non-cell-autonomous Activation of IL-6/STAT3 Signaling Mediates FGF19-driven Hepatocarcinogenesis. Nat Commun 8 : 15433, 2017
32. He G, Dhar D, Nakagawa H, Font-Burgada J, Ogata H, Jiang Y, Shalapour S, Seki E, Yost SE, Jepsen K : Identification of liver cancer progenitors whose malignant progression depends on autocrine IL-6 signaling. Cell 155 : 384-396, 2013
33. Porta C, Amici MD, Quaglini S, Paglino C, Tagliani F, Boncimino A, Moratti R, Corazza GR : Circulating interleukin-6 as a tumor marker for hepatocellular carcinoma. Ann Oncol 19 : 353-8, 2008
34. Wan S, Zhao E, Kryczek I, Vatan L, Sadovskaya A, Ludema G, Simeone DM, Zou W, Welling TH : Tumor-associated macrophages produce interleukin 6 and signal via STAT3 to promote expansion of human hepatocellular carcinoma stem cells. Gastroenterology 147 : 1393-404, 2014
35. Nawaz R, Zahid S, Idrees M, Rafique S, Shahid M, Ahad A, Amin I, Almas I, Afzal S : HCV-induced regulatory alterations of IL-1β, IL-6, TNF-α, and IFN-ϒ operative, leading liver en-route to non-alcoholic steatohepatitis. Inflamm Res 66 : 477-86, 2017
36. Brandi G, Lorenzo SD, Candela M, Pantaleo MA, Bellentani S, Tovoli F, Saccoccio G, Biasco G : Microbiota, NASH, HCC and the Potential Role of Probiotics. Carcinogenesis 38 : 231-40, 2017
37. Gupta H, Youn GS, Shin MJ, Suk KT : Role of Gut Microbiota in Hepatocarcinogenesis. Microorganisms 7 : 121, 2019
38. Takasu C, Wubetu GY, Kurita N, Yoshikawa K, Kashihara H, Kono T, Shimada M : TU-100 Exerts a Protective Effect Against Bacterial Translocation by Maintaining the Tight Junction. Surg Today 47 : 1287-94, 2017
39. Li L, Ma L, Fu P : Gut Microbiota-Derived Short-Chain Fatty Acids and Kidney Diseases. Drug Des Devel Ther 11 : 3531-42, 2017
40. Sasaki K, Sasaki D, Sasaki K, Nishidono Y, Yamamori A, Tanaka K, Kondo A : Growth stimulation of Bifidobacterium from human colon using daikenchuto in an in vitro model of human intestinal microbiota. Sci Rep 11 : 4580, 2021
41. Hasebe T, Ueno N, Musch MW, Nadimpalli A, Kaneko A, Kaifuchi N, Watanabe J, Yamamoto M, Kono T, Inaba Y : Daikenchuto (TU-100) shapes gut microbiota architecture and increases the production of ginsenoside metabolite compound K. Pharmacol Res Perspect 4 : e00215,2016. doi : 10.1002/prp2.215.
42. Tyler AD, Knox N, Kabakchiev B, Milgrom R, Kirsch R, Cohen Z, McLeod R, Guttman DS, Krause DO, Silverberg MS : Characterization of the gut-associated microbiome in inflammatory pouch complications following ileal pouch-anal anastomosis. PLoS One 8 : e66934, 2013
43. Furusawa Y, Obata Y, Fukuda S, Endo TA, Nakato G, Takahashi D, Nakanishi Y, Uetake C, Kato K, Kato T : Commensal microbe-derived butyrate induces the differentiation of colonic regulatory T cells. Nature 504 : 446-50, 2013
44. Kanwal R, Gupta K, Gupta S : Cancer epigenetics : an introduction. Methods Mol Biol 1238 : 3-25, 2015
45. Harris RA, Shah R, Hollister EB, Tronstad RR, Hovdenak N, Szigeti R, Versalovic J, Kellermayer R : Colonic Mucosal Epigenome and Microbiome Development in Children and Adolescents. J Immunol Res 2016 : 9170162, 2016
46. Del Chierico F, Nobili V, Vernocchi P, Russo A, Stefanis C, Gnani D, Fuelanello C, Zandona A, Paci P, Capuani G : Gut microbiota profiling of pediatric nonalcoholic fatty liver disease and obese patients unveiled by an integrated meta-omics-based approach. Hepatology 65 : 451-64, 2017
47. Brahe LK, Le Chatelier E, Prifti E, Pons N, Kennedy S, Hansen T, Pedersen O, Astrup A, Ehrlich SD, Larsen LH : Specific gut microbiota features and metabolic markers in postmenopausal women with obesity. Nutr Diabetes 5 : e159, 2015
48. Matsushita N, Osaka T, Haruta I, Ueshiba H, Yanagisawa N, Omori-Miyake M, Hashimoto E, Shibata N, Tokushige K, Saito K : Effect of Lipopolysaccharide on the Progression of Non-Alcoholic Fatty Liver Disease in High Caloric Diet-Fed Mice. Scand J Immunol 83 : 109-18, 2016
49. Huang R, Li T, Ni J, Bai X, Gao Y, Li Y, Zhang P, Gong Y : Different Sex-Based Responses of Gut Microbiota During the Development of Hepatocellular Carcinoma in Liver-Specific Tsc1-Knockout Mice. Front Microbiol 9 : 1008, 2018
50. Beringer A, Miossec P : IL-17 and TNF-α co-operation contributes to the proinflammatory response of hepatic stellate cells. Clin Exp Immunol 198 : 111-20, 2019
51. Ding NM, Xiao Y, Wu X, Zou H, Yang S, Shen Y, Xu J, Workman HC, Usborne AL, Hua H : Progression and Regression of Hepatic Lesions in a Mouse Model of NASH Induced by Dietary Intervention and Its Implications in Pharmacotherapy. Front Pharmacol 9 : 410, 2018